

This is the Accepted Version (post-peer-review, pre-copyedit) of

[S. Klein, C. Appert-Rolland, and L. Santen, *Environmental control of microtubule-based bidirectional cargo-transport*, EPL, **107** (2014) 18004]

The final published version is available online at:
<http://dx.doi.org/10.1209/0295-5075/107/18004>

Environmental control of microtubule-based bidirectional cargo transport

SARAH KLEIN^{1,2}, CÉCILE APPERT-ROLLAND¹ and LUDGER SANTEN²

¹ *Laboratory of Theoretical Physics, CNRS (UMR 8627), University Paris-Sud Bâtiment 210, F-91405 ORSAY Cedex, France*

² *Fachrichtung Theoretische Physik, Universität des Saarlandes D-66123 Saarbrücken, Germany*

PACS 87.16.Uv – Subcellular structure and processes - Active transport processes

PACS 87.16.Nn – Subcellular structure and processes - Motor proteins (myosin, kinesin dynein)

PACS 87.10.Mn – General theory and mathematical aspects - Stochastic modeling

Abstract – Inside cells, various cargos are transported by teams of molecular motors. Intriguingly, the motors involved generally have opposite pulling directions, and the resulting cargo dynamics is a biased stochastic motion. It is an open question how the cell can control this bias. Here we develop a model which takes explicitly into account the elastic coupling of the cargo with each motor. We show that bias can be simply controlled or even reversed in a counterintuitive manner via a change in the external force exerted on the cargo or a variation of the environmental properties. Furthermore, the superdiffusive behavior found at short time scales indicates the emergence of motor cooperation induced by cargo-mediated coupling.

Introduction. – In cells, most of the active transport processes, which are essential for cellular functions, are driven by molecular motors. These molecular motors are proteins having the ability to move preferentially in a defined direction on the polar filaments of the cytoskeleton [1]. The three most well-known molecular motors' families involved in transport are myosins, which move on actin filaments, dyneins and kinesins, which use microtubules (MT) as tracks [2]. Kinesin motors are stepping preferentially toward the growing (or plus-) end of MTs while dynein motors walk in the opposite direction.

Molecular motors can step individually or transport cargos along the cytoskeletal filaments. In order to generate forces large enough [3] to move a big cargo in the crowded environment of the cell, cargos are often transported by teams of molecular motors [4]. This is obviously beneficial if motors of the same type are attached to the cargo, since the force can be distributed between them. It enhances the processivity of the cargo and its ability to resist against forces emerging when transporting the cargo.

In many cases, however, motors that are attached to a given cargo pull in opposite preferential directions. Surprisingly, the attachment of two kinds of motors is not only observed for objects like mitochondria, which have to be spread out in the whole cell volume [5], but also for cargos which have a definite target, for example to be

transported from the cell center to the membrane or *vice versa* [6].

Although the attachment of two kinds of motors should enable bidirectional transport it is expected that, due to the difference in the characteristics of the various types of motors attached to the cargo [7] and possibly in the number of attached motors, the cargo undergoes a *biased* stochastic walk if the MT network is oriented.

Depending on the given motor-cargo system and the environment of the filaments different types of motion have been observed, which can be controlled by different mechanisms.

Some pigment cells (melanosomes) for example have the ability to switch between two states, in which the pigments are either dispersed or aggregated at one extremity of the filaments [8, 9]. The mechanisms that allow for such a transition from a non-biased to a biased motion are not yet well understood but have been related to signaling processes which regulate the activity of the attached motors [10].

Next to the active regulation of the motor dynamics, for example in cell signaling processes, also the cellular environment plays an important role. Recent *in vivo* experimental studies on cargos transported bidirectionally have revealed a very complex dynamical behavior. Super- as well as subdiffusive regimes of the cargos' trajectories

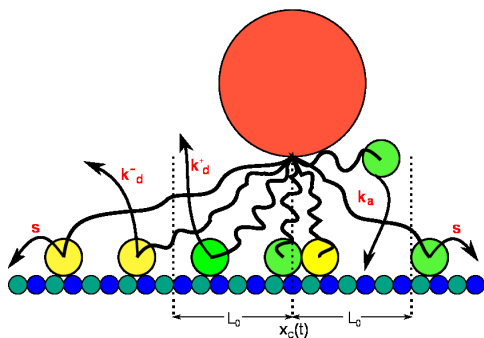


Fig. 1: Sketch of the model dynamics. The cargo (red) is pulled by two families of molecular motors (yellow and green) hopping in opposite directions on the MT.

have been identified [11–13]. Bidirectional cargo transport on MT networks has also been studied *in vitro* where enhanced diffusion was obtained as well [14].

It was also observed that a change in direction often occurs due to cellular obstacles like other cargos or the cytoskeleton itself [15]. In order to disentangle the action of different external control mechanisms on motor-cargo complexes we study their dynamics by means of a theoretical model.

Several approaches have been proposed in the past years to describe cargo transport mediated by one [16–18] or two types of motors [7, 19, 20]. The stochastic model we introduce in this work which is similar to the one in [7] describes bidirectional cargo-motion along microtubules driven by teams of kinesin and dynein motors. We will show that a variation of the environment changes the cargo-dynamics in a non-trivial way and can even invert the direction of the bias. A non-trivial response to the effective viscosity of the environment (representing the crowdedness of the surrounding cytoskeleton) is also obtained as a result of the complex interaction between the attached molecular motors. Additionally, we show that, as observed in several *in vivo* experiments [12, 13], super-diffusive particle motion can be observed in our model.

Model. – We introduce a stochastic model for the transport of a cargo by teams of molecular motors along a single microtubule. In our model, which is inspired by the bidirectional cargo transport models of [7, 19], N_+ and N_- motors are tightly bound to the cargo and pull it in plus- and minus-direction, respectively. Throughout the paper we shall take $N_+ = N_- = 5$ if not stated otherwise. In contrast to [19] we take every single motor position x_i into account and calculate the thereby generated force F_i on the cargo as in [7]. We model the tail of the molecular motors, which permanently connects the motor domain with the cargo, as a linear spring with untensioned length L_0 and spring constant α (Fig. 1). The motors can perform three different actions: if they are bound to the filament, which is represented as a one-dimensional lattice, they can make a step of size d or detach from the fila-

ment. Both events occur with force-dependent rates $s(F_i)$ and $k_d^\pm(F_i)$, respectively. Once a motor has detached from the filament, it can reattach in the interval $\pm L_0$ around the cargo’s center of mass with a force-independent rate k_a . Due to the de-/attachment events the number of plus (minus) motors bound to the filament is in the range $0 \leq n_+ \leq N_+$ ($0 \leq n_- \leq N_-$). The resulting force on the cargo at position $x_C(t)$ at time t is then given by the sum of all single forces applied by bound motors

$$F(x_C(t), \{x_i\}) = \sum_{i=1}^{n_+ + n_-} F_i(x_i - x_C(t)) \quad (1)$$

with

$$F_i(x_i - x_C(t)) = \begin{cases} \alpha(x_i - x_C(t) + L_0), & x_i - x_C(t) < -L_0 \\ 0, & |x_i - x_C(t)| < L_0 \\ \alpha(x_i - x_C(t) - L_0), & x_i - x_C(t) > L_0 \end{cases} \quad (2)$$

The motor’s stepping behavior depends on the surrounding ATP concentration ($[ATP]$) as well as the force F_i applied to the cargo. As mentioned above, forces that are acting on the motors change their detachment and stepping rate. If the force is acting against the preferred direction the motor may slow down, stop or even invert its direction. The maximal force (in absolute value) under which a motor still walks in its preferred direction is given by F_S . We shall thus distinguish two regimes for the stepping behavior, depending on whether the applied force is smaller than the stall force (regime I) or larger (regime II). In regime I (+end motors: $0 \leq F_i < F_S$; -end motors: $-F_S < F_i \leq 0$), we use a 2-state Michaelis-Menten equation which was introduced in [21] to model kinesin stepping: we describe the motor stepping rate with ATP playing the role of the stepping catalyst. On the one hand we have ATP which is needed to convert the chemical energy in mechanical energy to perform a step, on the other hand we have the force which acts on the motor and reduces its stepping rate. So we use

$$s(F_i, [ATP]) = \frac{k_{\text{cat}}(F_i)[ATP]}{[ATP] + k_{\text{cat}}(F_i) \cdot k_b(F_i)^{-1}}, \quad (3)$$

where k_{cat} is the rate constant for the ATP catalysis, k_b is a second-order rate constant for ATP binding. Both rate constants depend on the load force. As the stepping rate decreases with increasing absolute force $|F_i|$, $k_b(|F_i|)$ declines faster with force than $k_{\text{cat}}(|F_i|)$. Schnitzer *et al.* [21] introduce a Boltzmann-type force relation for the rate constants

$$k_j(F_i) = \frac{k_j^0}{p_j + q_j \exp(\beta F_i \Delta)} \quad j = \{\text{cat}, \text{b}\} \quad (4)$$

with a constant k_j , $p_j + q_j = 1$, $\beta = (k_b T)^{-1}$ and Δ which is the characteristic distance over which the load

acts. It was measured for kinesin [21] and dynein [22] that the stepping rate, depending on [ATP] and the load force F_i , can be described by eq. (3). The ATP-concentration can be varied considerably in *in vitro* experiments while *in vivo* processes other than the motors' stepping rates would be influenced as well.

It is not conclusively clarified whether the stall force of kinesin and dynein depends on [ATP] or not. Following the experimental results of [2] we choose dynein's stall force changing with [ATP] in an affine linear manner from $F_S([ATP] = 0 \text{ mM}) = 0.3 \text{ pN}$ to $F_S([ATP] = 1 \text{ mM}) = 1.2 \text{ pN}$ where it saturates, while we leave kinesin's stall force constant at 2.6 pN . This determines Δ as given in in Table 1 to ensure that the stepping rate is zero at stall. We find Δ to get $s(F_S) \ll 1$ by solving the equation

$$\frac{k_{\text{cat}}(F_S)[ATP]}{[ATP] + k_{\text{cat}}(F_S) \cdot k_b(F_S)^{-1}} = 10^{-13} \text{ s}^{-1}, \quad (5)$$

where we use k_{cat}^0 , k_b^0 , q_{cat} and q_b from Schnitzer *et al.* [21] and given in Table 1 to define the stepping rate $s(|F_i|, [ATP])$. In regime II (+end motors: $F_i \geq F_S$; -end motors: $-F_S \geq F_i$), the motors can walk backwards with the constant rate

$$s(F_i) = \frac{v_b}{d}, \quad (6)$$

corresponding to the backward velocity v_b , which is at least one order smaller than the force-free forward velocity. In the model we neglect any motor position exclusion on the filament since motors can walk on several lanes of the microtubule. Furthermore the MT network is very dense in many cell regions, as for example in axons where the distance between two microtubules is about 20 nm [30]. There, motors can walk on multiple microtubules around the pulled cargo. We choose the detachment behavior according to [7]

$$k_d^+(F_i) = \begin{cases} k_d^0 \exp\left(\frac{|F_i|}{2.5f}\right) & F_i < F_S \\ k_d^0 \left(0.186 \frac{|F_i|}{f} + 1.535\right) & F_i \geq F_S \end{cases} \quad (7)$$

for kinesin and

$$k_d^-(F_i) = \begin{cases} k_d^0 \exp\left(\frac{|F_i|}{2.5f}\right) & F_i > -F_S \\ k_d^0 \left[1.5 \left(1 - \exp\left(\frac{-|F_i|}{1.97f}\right)\right)\right]^{-1} & F_i \leq -F_S \end{cases} \quad (8)$$

for dynein. We use the force-free detachment rate k_d^0 and a standardization force $f = 1 \text{ pN}$ which determines the force scale. Note that the behavior of both types of motors differs above stall, where we have a catch-bond like rate (decreasing with F_i) for dynein. We propagate the system by means of Gillespie's algorithm for time-dependent rates [31], since the force exerted on each motor (and thus the rates) is time-dependent. The viscosity η of the cytoskeleton is taken into account when we solve the equation of motion for the cargo

$$m \frac{\partial^2 x_C(t)}{\partial t^2} = -\beta \frac{\partial x_C(t)}{\partial t} + F(x_C(t), \{x_i\}), \quad (9)$$

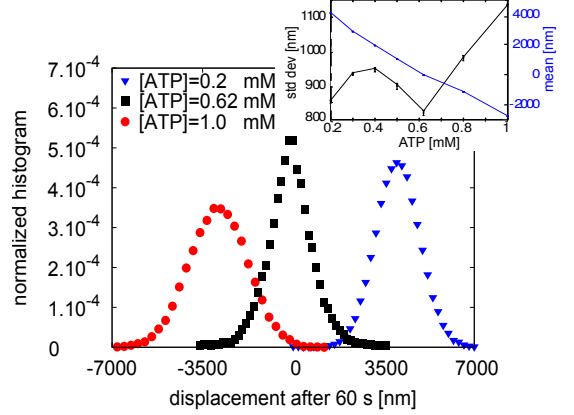


Fig. 2: Normalized histogram of the displacement after 60 s of cargo propagation. The red circles correspond to [ATP]=0.2 mM, the black squares to [ATP]=0.62 mM and the blue triangles to [ATP]=1.0 mM. We get for the mean displacement $\mu_{0.2} = 4028.3 \pm 1.14 \text{ nm}$ and the standard deviation $\sigma_{0.2} = 855.9 \pm 1.13 \text{ nm}$ for [ATP] = 0.2 mM, $\mu_{1.0} = -2887.5 \pm 3.17 \text{ nm}$ and $\sigma_{1.0} = 1139.9 \pm 2.59 \text{ nm}$ for [ATP] = 1.0 mM and $\mu_{0.62} = -27.8 \pm 14.08 \text{ nm}$ and $\sigma_{0.62} = 836.9 \pm 11.5 \text{ nm}$ for [ATP] = 0.62 mM. Obviously, the displacement changes direction from plus-end bias for stronger plus motors at low [ATP] to minus-end bias at saturating [ATP]. The inset shows the non-monotonous curve of the standard deviation of the displacement (black) against the ATP concentration while the mean displacement (blue) decreases monotonously.

with Stokes' law $\beta = 6\pi\eta R$ (R : cargo radius, m : cargo's mass).

Results and Discussion. – First we simulate the model in order to measure the distribution of the cargo displacement for one-minute intervals (see Fig. 2). The results, which we obtained for the model's parameters given in Table 1, show that we can tune the mean velocity (or bias) of the transported cargo continuously by means of the ATP-concentration. Remarkably, the cargo *slows down with increasing* ATP-concentration until the bias vanishes (at an ATP concentration of 0.62 mM for our choice of the parameters). For larger concentrations of ATP the bias is inverted and its absolute value increases again. In contrast to scenarios based on signaling processes where a protein would up- or down-regulate only one motor species, here the inversion of the bias results from the difference in the [ATP] dependence of both motors' activities. In particular dynein detaches more easily with decreasing ATP concentration and so the bias is then directed to the plus-end. We also notice that an unbiased motion of the cargo can only be obtained in a rather narrow interval of ATP-concentration, so that biased motion is generic. The step rate of the motors depend not only on the ATP concentration but also on the force which is applied to the motor. The external force applied to the moving cargo can be parametrized via the viscosity of the environment. In Fig. 3 we show the dependence

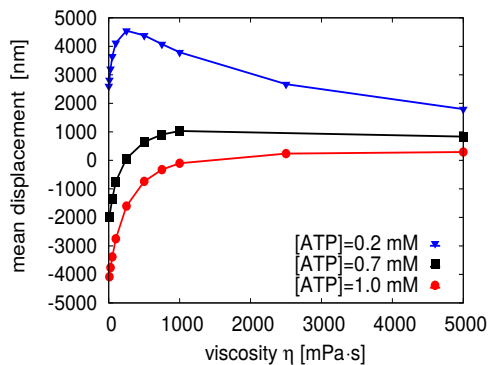


Fig. 3: Mean displacement after 60 s of cargo propagation for different cytoskeleton viscosities η . The red circles corresponds to the $[ATP]=0.2$ mM, the black squares to $[ATP]=0.7$ mM and the blue triangles to $[ATP]=1.0$ mM. For small $[ATP]$ the mean displacement-viscosity relation shows a non-monotonous behavior. In the case of $[ATP]=0.7$ mM we observe a change in direction with increasing viscosity.

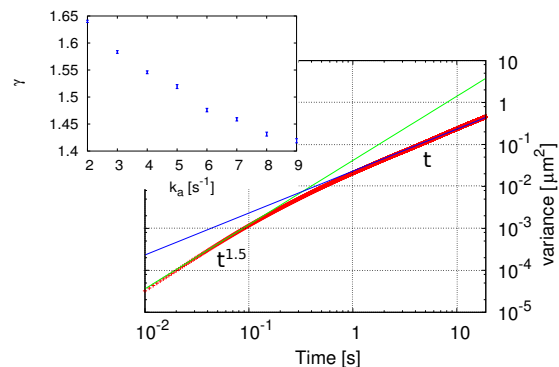


Fig. 4: Variance of the numerically generated trajectories with $[ATP]=1$ mM. One observes at 0.5 s a crossover from enhanced diffusion going with t^γ , $\gamma = 1.5$ (green line) to normal diffusion proportional to t with a diffusion coefficient $D = 0.04 \mu\text{m}^2\text{s}^{-1}$ (blue line). The inset shows how the exponent varies with the attachment rate k_a .

of the mean displacement on the viscosity (for different ATP concentrations). We observe a non-trivial dependence of the bias on the viscosity. Counterintuitively, the absolute value of the bias can increase with increasing viscosity. For intermediate ATP concentrations (see, e.g., 0.7 mM in Fig. 3) one observes that the cargo is changing its direction with increasing viscosity. This effect can be used in order to leave crowded areas in the cellular environment, which correspond to high effective viscosities, and enhance thereby the efficiency of the motor-driven transport. Here we find the bias-inversion regime for a limited range of $[ATP]$. Depending on the cargo and the transportation task to be fulfilled it could be more favorable to be in this bias-inversion regime or in a regime of strong bias. Evolution could have selected the regime by adjusting some other parameters like the motors concentration or an asymmetry in the motor properties. Indeed, a change in N_+ , N_- modifies the values of the external control parameters at which we observe the reversal of the bias. The cargo-mediated coupling of the engaged motors induces a time-correlated motion of the cargo. These correlations lead to non-gaussian displacement distributions of the cargo at short finite time intervals (see Fig. 2). The range of the correlations can be estimated from the functional behavior of the cargo's variance

$$\text{Var}[x_C(t)] = \langle x_C(t)^2 \rangle - \langle x_C(t) \rangle^2. \quad (10)$$

Unlike in most experiments we chose the variance instead of the mean square displacement. This enables us to disentangle correlation effects from non-diffusive behavior that originates from the bias of the motor-cargo complex. Thus by measuring the variance we are able to analyze if our model exhibits a persistent motion with a (finite) correlation time. Indeed, our simulation results show a transition from enhanced diffusion at short times to normal diffusion. For the set of parameters of Table 1 we observe that the

variance is growing as $t^{1.5}$ at short time scales. Thus, our model generates a superdiffusive behavior which indicates cooperation between motors induced by cargo-mediated coupling. Our results also show that the exponent is not universal (inset Fig. 4). By varying the attachment rate, which depends strongly on the cellular environment, we have been able to observe exponents between 1.4 and 1.6, so in the same range as observed experimentally [11, 12].

Asymptotically we observe purely (biased or unbiased) diffusive behavior. This asymptotic diffusive regime is generic for our model as long as we assume cargo motion on a single filament. By contrast, on a branched microtubule network the asymptotic behavior may be influenced by the structure of the network as shown in the case of the microtubule-network of giant fibroblast [12], where sub-diffusive behavior has been observed.

Influence of the model parameter. We want to analyze the influence of the model parameters on the system's dynamics more in detail. We shall now vary one single parameter at a time. The other parameters will keep their value of Table 1, while two values for $[ATP]$ will be considered (0.2 and 1 mM) corresponding to a positive and negative cargo bias, respectively.

First we vary the total number of motors while keeping $N_+ = N_-$. We observe that the cargo slows down with increasing motor number and the absolute value of the average bias decreases. One can explain this effect by taking a close look to the motor configuration.

Motors always attach to the microtubule in the force-free area $x_C(t) \pm L_0$, and it takes some time before they can apply a force on the cargo. The set of these non-pulling attached motors can be seen as a *reservoir* of motors that can be mobilised very quickly when the configuration of pulling motors changes, as illustrated in Fig. 5: when a pulling motor detaches, the cargo moves and new motors from the *reservoir* are involved in the tug-of-war. During this process, the more motors there are in the *reservoir*,

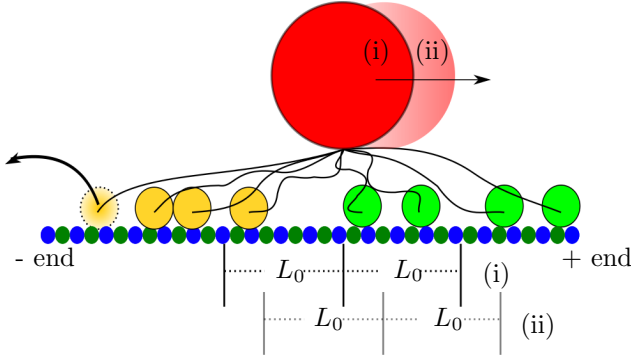


Fig. 5: Sketch of the motor *reservoir*. Assuming that four motors of both kinds are bound to the filament in the given configuration, three minus-end directed motors (yellow) and two plus-end directed motors (green) pull the cargo. If the leftmost motor detaches, the cargo will move to the right and therewith also the area of untensioned motors $x_C(t) \pm L_0$ (going from state (i) to (ii)). In the new motor configuration still three minus-end directed motors and two plus-end directed motors exert a force on the cargo.

the more limited the displacement of the cargo is.

The above argument involves only motors attached to the microtubule. Another way to increase this number is to increase the attachment rate k_a . Then the bias should decrease. Conversely, increasing the *detachment rate* k_d^0 should lower the number of attached motors and thus increase the bias. This is what is indeed observed in our simulations.

Eventually, if we increase the *force-free velocity* v_f , the absolute value of the bias increases for both $[ATP]$ values. Indeed, motors will then exit the force-free area more rapidly, depleting the *reservoir* of non-pulling attached motors.

Conclusion. – In this work we study the effect of environmental features on cargos transported by teams of motors.

We find that trajectories of such motor-cargo complexes exhibit different dynamic regimes. Generically one observes a biased motion of the cargo, since the activity of dynein and kinesin motors can only be balanced in a very narrow interval of the external control parameters (here viscosity and ATP-concentration). The mechanical coupling of the motors induces time-correlated cargo trajectories. In the comoving frame, the correlations lead to super-diffusive behavior at short times. The exponents which describe the time evolution of the variance at short times, as well as the time at which one observes the transition to gaussian displacement distributions are parameter-dependent. For typical parameter combinations the crossover to diffusion takes place at time intervals of the order of one second. Here we have not considered thermal fluctuations. On-going work shows that thermal noise is only relevant for time scales even smaller than those of Fig. 4 and does not alter the superdiffusion.

Naively one would expect faster cargo transport for higher concentrations of ATP and lower viscosities. In this work we show that this is not the case. The response to both environmental parameters is non-monotonous. Counterintuitively, the cargo may accelerate with increasing viscosity for a given parameter-range. We also find an unexpected response of the cargo dynamics to variation of the ATP concentration. We not only observe a change of the bias but also a non-monotonous dependence of the width of the displacement distribution on the ATP concentration. The recent progress in dynein motility assays allows now to test our predictions *in vitro*. The realization of such *in vitro* assays would allow to study the mechanic coupling of molecular motors via the cargo in a much simpler environment as in the living cell. *In vivo* we do not expect relevant variations of ATP concentration. However, the ATP hydrolysis could be locally regulated at the level of motors.

In crowded areas of the cell, interactions between different cargos as well as between cargo and filament may apply forces on the molecular motors. Our model results show that, since kinesin and dynein motors respond differently to external forces, this may lead to an inversion of the cargo's bias, even if no distinct control mechanism is applied. The ability of the cargo to change its direction in a crowded environment, i.e. an environment of higher effective viscosity, may give an argument why the transport of cargo by oppositely directed motors can be beneficial for the cell.

This work was supported by the Deutsche Forschungsgemeinschaft (SFB1027,GRK1276) and the BMBF (FKZ 03X0100C).

REFERENCES

- [1] ALBERTS B., JOHNSON A., LEWIS J., RAFF M., ROBERTS K. and WALTER P., *Molecular biology of the cell* 4th Edition (Garland Science Taylor & Francis Group) 2002.
- [2] MALLIK R. and GROSS S. P., *Current Biology*, **14** (2004) R971 .
- [3] CHOWDHURY D., *Physics Reports*, **529** (2013) 1.
- [4] KURAL C., KIM H., SYED S., GOSHIMA G., GELFAND V. I. and SELVIN P. R., *Science*, **308** (2005) 1469.
- [5] HOLLENBECK P. J. and SAXTON W. M., *Journal of cell science*, **118** (2005) 5411.
- [6] WELTE M. A., *Current Biology*, **14** (2004) R525.
- [7] KUNWAR A., TRIPATHY S. K., XU J., MATTSON M. K., ANAND P., SIGUA R., VERSHININ M., MCKENNEY R. J., YU C. C., MOGILNER A. and GROSS S. P., *Proceedings of the National Academy of Sciences*, **108** (2011) 18960.
- [8] GROSS S. P., TUMA M. C., DEACON S. W., SERPINSKAYA A. S., REILEIN A. R. and GELFAND V. I., *The Journal of Cell Biology*, **156** (2002) 855.
- [9] NASCIMENTO A. A., ROLAND J. T. and GELFAND V. I., *Annual Review of Cell and Developmental Biology*, **19** (2003) 469.

	kinesin	dynein	Ref.
d	8 nm		[22, 23]
N_{\pm}	5		[24]
v_f	1000 nm/s		[22, 23]
v_b	6 nm/s		[23, 25]*
α	0.1 pN/nm		[7]*
k_a	5 s^{-1}		[19, 26]
k_d^0	5 s^{-1}		[7]*
f	1 pN		
F_S	2.6 pN	0.3-1.2 pN	[27, 28]
$k_d(F)$	$\begin{cases} k_d^0 \exp\left(\frac{ F }{F_D}\right), & F < F_S \\ k_d^0(1.535 + 0.186 \cdot \frac{ F }{f}), & F \geq F_S \end{cases}$	$\begin{cases} k_d^0 \exp\left(\frac{ F }{F_D}\right), & F > -F_S \\ k_d^0 \left[1.5 \left(1 - \exp\left(\frac{- F }{1.97f}\right)\right)\right]^{-1}, & F \leq -F_S \end{cases}$	[7]*
k_{cat}^0	$v_f \cdot d^{-1}$		[21]
k_b^0	$1.3 \mu\text{M}^{-1}\text{s}^{-1}$		[21]
q_{cat}	$6.2 \cdot 10^{-3}$		[21]
q_b	$4 \cdot 10^{-2}$		[21]
Δ	4267.3 nm	$\max\left(\frac{2.9 \cdot 10^5}{[\text{ATP}]^{0.3}} - 28111.1, 8534.6\right)$ nm	eq. (5)
Environment			
η	100 mPa·s		[11]*
Cargo			
R	250 nm		[29]*
m	$5 \cdot 10^{-19} - 5 \cdot 10^{-17}$ kg		

Table 1: The second and third column show the simulation parameters for kinesin and dynein, respectively. The fourth column gives the references providing experimental basis to these values. The * indicates that the experimental support gives the order of magnitude only.

- [10] NILSSON SKÖLD H., ASPENGREN S. and WALLIN M., *Pigment cell & melanoma research*, **26** (2013) 29.
- [11] KULIĆ I. M., BROWN A. E., KIM H., KURAL C., BLEHM B., SELVIN P. R., NELSON P. C. and GELFAND V. I., *Proceedings of the National Academy of Sciences*, **105** (2008) 10011.
- [12] CASPI A., GRANER R. and ELBAUM M., *Physical Review E*, **66** (2002) 011916.
- [13] ROBERT D., NGUYEN T.-H., GALLET F. and WILHELM C., *PloS one*, **5** (2010) e10046.
- [14] SALMAN H., GIL Y., GRANER R. and ELBAUM M., *Chemical physics*, **284** (2002) 389.
- [15] BRUNO L., ECHARTE M. M. and LEVI V., *Cell biochemistry and biophysics*, **52** (2008) 191.
- [16] KUNWAR A., VERSHININ M., XU J. and GROSS S. P., *Current biology*, **18** (2008) 1173.
- [17] KORN C. B., KLUMPP S., LIPOWSKY R. and SCHWARZ U. S., *The Journal of chemical physics*, **131** (2009) 245107.
- [18] BERGER F., KELLER C., KLUMPP S. and LIPOWSKY R., *Physical review letters*, **108** (2012) 208101.
- [19] MÜLLER M. J. I., KLUMPP S. and LIPOWSKY R., *Proceedings of the National Academy of Sciences*, **105** (2008) 4609.
- [20] ZHANG Y., *Physical Review E*, **87** (2013) 052705.
- [21] SCHNITZER M. J., VISSCHER K. and BLOCK S. M., *Nat Cell Biol*, **2** (2000) 718.
- [22] TOBA S., WATANABE T. M., YAMAGUCHI-OKIMOTO L., TOYOSHIMA Y. Y. and HIGUCHI H., *Proceedings of the National Academy of Sciences*, **103** (2006) 5741.
- [23] CARTER N. J. and CROSS R. A., *Nature*, **435** (2005) 308.
- [24] WELTE M. A., GROSS S. P., POSTNER M., BLOCK S. M. and WIESCHAUS E. F., *Cell*, **92** (1998) 547.
- [25] GENNERICH A., CARTER A. P., RECK-PETERSON S. L. and VALE R. D., *Cell*, **131** (2007) 952.
- [26] LEDUC C., CAMPÀS O., ZELDOVICH K. B., ROUX A., JOLIMAITRE P., BOUREL-BONNET L., GOUD B., JOANNY J.-F., BASSEREAU P. and PROST J., *Proceedings of the National Academy of Sciences of the United States of America*, **101** (2004) 17096.
- [27] MALLIK R., CARTER B. C., LEX S. A., KING S. J. and GROSS S. P., *Nature*, **427** (2004) 649.
- [28] SHUBEITA G. T., TRAN S. L., XU J., VERSHININ M., CERMELLI S., COTTON S. L., WELTE M. A. and GROSS S. P., *Cell*, **135** (2008) 1098.
- [29] THIAM A. R., FARESE JR R. V. and WALTHER T. C., *Nature Reviews Molecular Cell Biology*, **14** (2013) 775.
- [30] HIROKAWA N., NODA Y. and OKADA Y., *Current Opinion in Cell Biology*, **10** (1998) 60.
- [31] GILLESPIE D. T., *Journal of Computational Physics*, **28** (1978) 395.